

EDDY CURRENT PROBE EVALUATION:

EXPERIMENTAL MEASUREMENTS AND SYSTEM INTERACTION

K.H. Hedengren, R.O. McCary and J.D. Young
Corporate Research and Development Center
General Electric Company
Schenectady, NY 12301

INTRODUCTION

Eddy current testing is often considered an old and mature technology. However, the state of the art technology cannot meet the new stringent demands that the US Government has imposed on inspection of new aircraft engines under a program called ENSIP (engine structural integrity program). These demands require substantial improvements both in inspection sensitivity and speed — for instance, crack detection capability must improve by a factor of 3 over what is currently possible. In order to meet the new goals, all aspects of an eddy current inspection system must be addressed from probe selection and mechanical scanning noise to system electronics and signal processing. It has previously been shown [1,2] that imaging techniques provide improved flaw detection capability and also may be used to optimize system performance. This paper describes work that combines imaging with probe measurements to analyze eddy current probes and system performance from a practical point of view. Slightly different designs of a specific type of probe have been examined to evaluate differences in the designs and to determine how well the probe construction method is controlled. Parameters were calculated from electric measurements on the probes and plotted in an attempt to explain their significance and to provide a method for selection of probes with superior qualities. The probe/system interaction was also analyzed in order to learn why some probes with good electric properties did not perform well in the eddy current system. Finally, images were created and used to evaluate the impact of different imaging parameters on inspection performance.

EDDY CURRENT INSPECTION SYSTEM

The block diagram in Figure 1 shows the similarities and differences between a state of the art eddy current inspection system and an advanced inspection system. A mechanical scanner moves either the probe or the part to collect data and electronics then process those data. Today, probes are calibrated by scanning standard specimens before they are used to inspect parts. A pre-selected threshold is applied to only one of the two eddy current signal components for defect detection. If an indication is found, the spatial location and amplitude of the signal are recorded in computer memory and the part is later manually examined at that position. The present method of inspection is quite primitive and lags behind other inspection technologies in sophistication. An advanced inspection system is based on image creation which requires additional hardware and special procedures for collecting, formatting, and saving the data. However, the image format provides correlated information in two

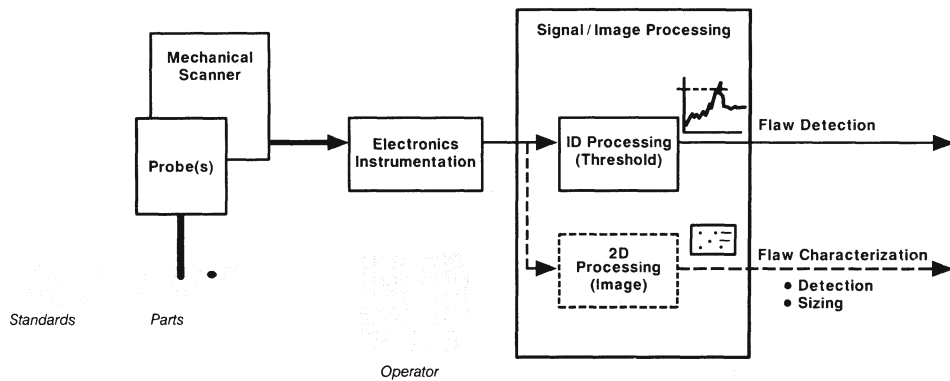


Figure 1. Eddy Current Inspection System

dimensions to enable spatial processing which, in turn, improves signal to noise and also improves the capability of characterizing defects with respect to size etc.

In order to enhance the inspection process so that it can meet the new requirements, it is necessary to look at the complete inspection system and identify how different components of the system limit the performance. The surface finish of the part itself, variability in probe quality, mechanical scanning noise, non-linearities and noise in the electronic instrumentation, and signal processing all affect the final inspection results. In addition, system integration may produce specific conditions (such as resonance effects) that can greatly reduce performance. Finally, it is well known that subjective judgments of human inspectors cause great variability of the inspection results. These issues must be dealt with one at a time in decreasing order of greatest source of error. The ultimate goal is to remove the effects of probes, scanner, electronics, and the system itself and reduce the inspection challenge to just a material/defect analysis.

ELECTRIC MEASUREMENTS ON PROBES

Split core differential probes

Eddy current probes are simply coils that are excited by alternating currents at some appropriate frequency. Probes may be designed with desired characteristics by combining two or more specific coils and by having the coils enclose and/or be surrounded by ferrite. The split core differential probe is a common type of probe which consists of two coils that are connected in a bridge circuitry so that the difference between the voltages across the two coils is recorded — thus the signal is zero if the probe is placed on a uniform metal surface and the two coils are electrically identical. Figure 2 shows three slightly different designs of the split core differential type of probe. The active region consists of two adjacent coils enclosed by a ferrite casing with each coil wound around a D-shaped ferrite core. For historic reasons, the coils are referred to as test and reference coils. A visual difference between the three probe designs is the depth placement of the coils. The question is how to quantitatively evaluate which probe design is best and which construction method is best controlled.

Probe measurements

A Hewlett-Packard 4194A Impedance Analyzer was used to measure electric parameters of the probe coils. In order to have a quick and semi-automatic method of measuring numerous

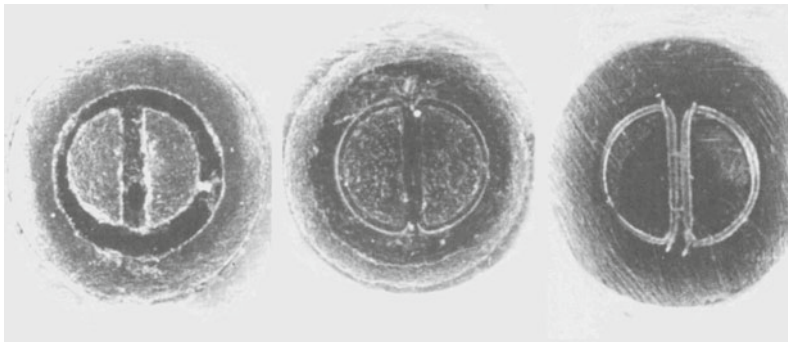


Figure 2. Split Core Differential Probe Designs

probes, a box containing special circuitry was built and connected directly to the HP analyzer. Inductance and resistance measurements at 2MHz were made of the probe coils individually, connected in series, and connected in parallel. In addition, coil impedances and phase angles were measured separately (also at 2 MHz) in air as well as with the probes touching material samples. These measurements were evaluated separately or were used to calculate and plot additional parameters. In the plots shown in this paper, the different probe designs are indicated by markers in the shapes of squares (A), circles (B), and triangles (C) corresponding to the probe designs from the left to the right in Figure 2. A total of 34 probes were measured: 8 of design A, 11 of design B and 15 of design C.

Figure 3 is a plot of the test coil versus reference coil impedances to demonstrate how well the two coils are matched in the same probe and also what the differences are between all the probes. If the two coils are identical, their impedances would be the same so, ideally, their marker should fall on the 45 degree line. The closer to the 45 degree line a marker is, the better matched the coils of the corresponding probe are. If the impedances of the coils within each type of design are carefully controlled, their markers would cluster close together. As can be seen, for design C (triangles) the coils are matched well for individual probes, but the probe to probe variation is large. The circles of design B cluster most tightly, but individual probes have some substantial coil mismatches. Design A (squares) show both poor match of the probe coils and large probe to probe variation.

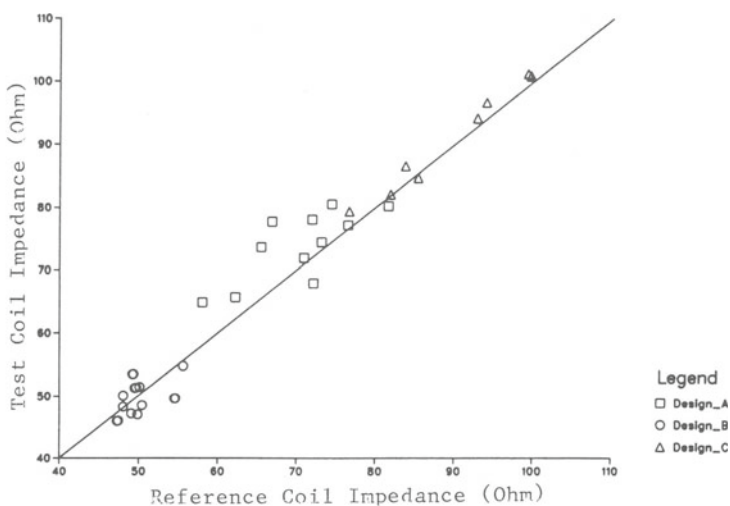


Figure 3. Probe Coil Matching

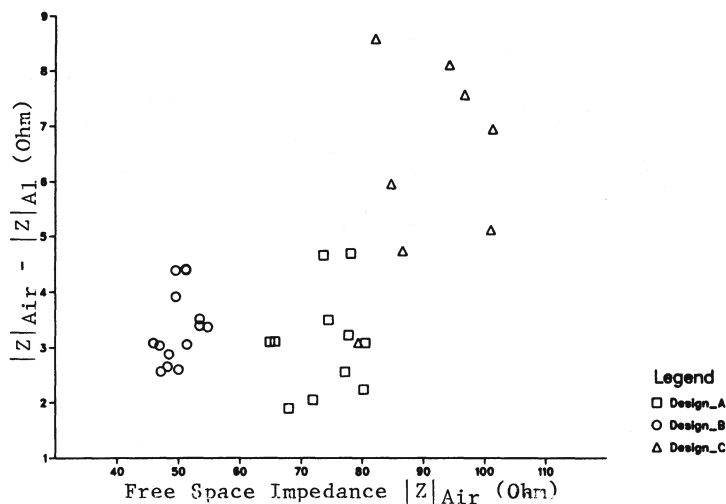


Figure 4. Probe Sensitivity

The difference between the free space impedance (probe in air) and the loaded impedance (probe in contact with material) is a measure of the probe sensitivity — the greater this difference is the better the probe will detect small surface breaking defects in the material. Figure 4 shows the probe sensitivities on Aluminum. Probes cluster together for each design but spread differently — design B probes should provide the most uniform results. Probes of design A are shown to be the least sensitive. This result correlates with the observation about Figure 2 that the coils are most recessed for that design.

The magnetic field produced by split core probes depends on whether the coils are connected in series or in parallel. A magnetic coupling coefficient between two split core coils can be computed as a function of the inductances of the coils connected in series and in parallel. The sign of this coefficient distinguishes between probes connected as split core differential (SCD) and recording head differential (RHD). Figure 5 is a bar plot of the magnetic coupling coefficients by probe design. It shows that probe design C is RHD whereas designs A and B are SCD. In addition, one probe of design A is shown to be connected differently from the others because its coupling coefficient has the wrong sign and one probe of design B is different from the others of that design. The sensitivity seems to be comparable for SCD and RHD designs with this particular probe geometry.

Figure 6 is a different way to represent magnetic coupling coefficient data. The dashed line corresponds to a coefficient of zero. Probes that fall above this line are connected RHD while probes below are SCD. The three probe designs separate very well and unknown probes could be sorted by type using this plot. It is also clear from the plot that the manufacturing process for design B produces the most uniform probes. With a large probe data base, one should be able to determine and indicate acceptable limits for variation of probe parameters for each specific design and use those for vendor specification and quality control.

EDDY CURRENT IMAGING

As has previously been reported [1,2], imaging techniques provide eddy current NDT with powerful new capabilities. Images are formed by scanning an object, usually in a raster fashion, measuring a physical parameter point by point and storing the measured values in

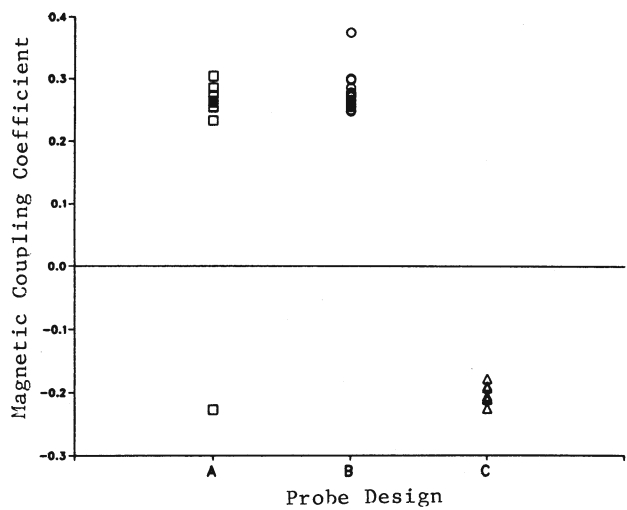


Figure 5. Magnetic Coupling Coefficients

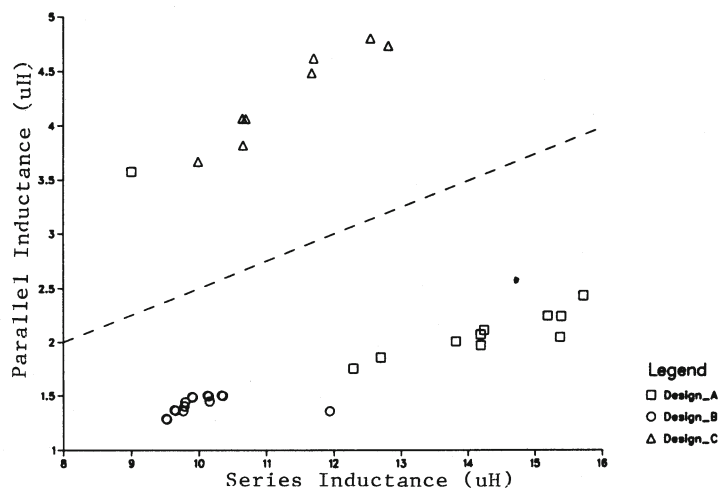


Figure 6. Probe Quality Control

an array. For eddy current images we measure electric impedance. Figure 7a shows signal amplitudes displayed by the perspective mountains and valleys. It also shows the intensities mapped into gray levels according to the gray scale to form images with black being the lowest signal amplitude and white being the highest. Pseudo-color images are created when a color scale is used instead of the gray scale.

Eddy current probes are physical coils and cannot be made infinitely small. Such probes, therefore, have large active areas. Because an eddy current image of a defect represents convolution of the active area of the probe with the shape of the defect, the image of the defect becomes very blurred. An image of a very small hole, therefore, is a footprint of the probe (i.e. the active area of the probe or the point spread function). Figure 7b shows footprints of an absolute probe, a recording head probe, a split core differential probe, and a four-coil probe.

Eddy current inspections are often performed on bolt holes in turbine disks because small cracks may appear near the edges. Figure 8 shows how a bolt hole is imaged and what the

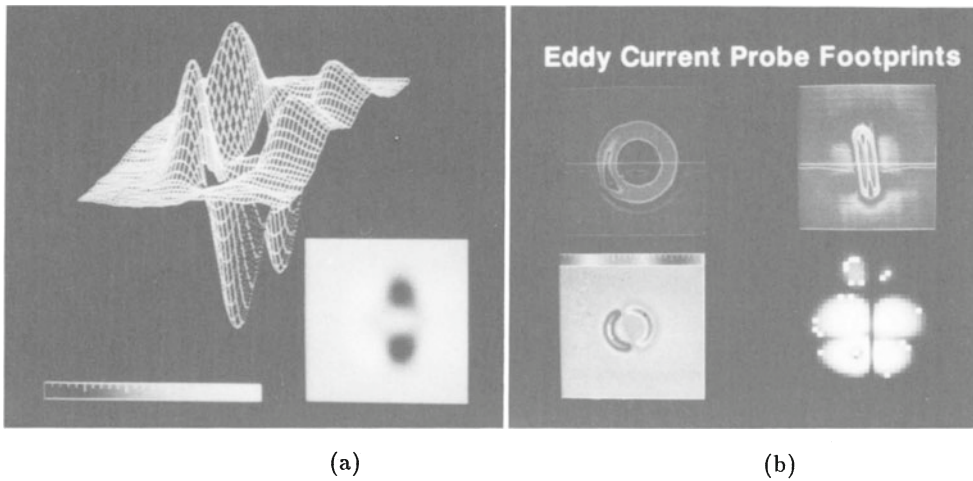


Figure 7. Eddy current (a)perspective and gray level images (b)foot-prints

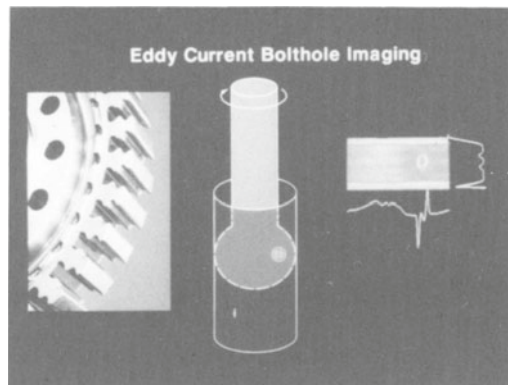


Figure 8. Bolthole imaging

image of a small defect looks like. In order to create an image, a probe that fits snugly in the bolt hole and has a small active element is rotated inside the bolt hole to collect data along the perimeter. After each rotation, the probe is moved downwards a small increment until the depth of the hole has been scanned. Thus, each rotation provides one line of data for the image. The traces below and to the side of the image represent the voltage levels along the horizontal and vertical lines that intersect at the center of the defect.

PROBE/SYSTEM EXPERIMENTS

Probe/system operating frequency

Even though a probe with excellent electric qualities is selected, it may not perform well in the imaging system. If this is the case, it may be well worthwhile to analyze specific probe/system characteristics. If a probe is attached to the eddy current system with a long cable, the resonance frequency will drop due to the added capacitance of the cable and undesirable conditions may occur. The example in Figure 9 shows what happens if the cable has about the same length as a quarter of the wavelength for a system operating at 2 MHz. The

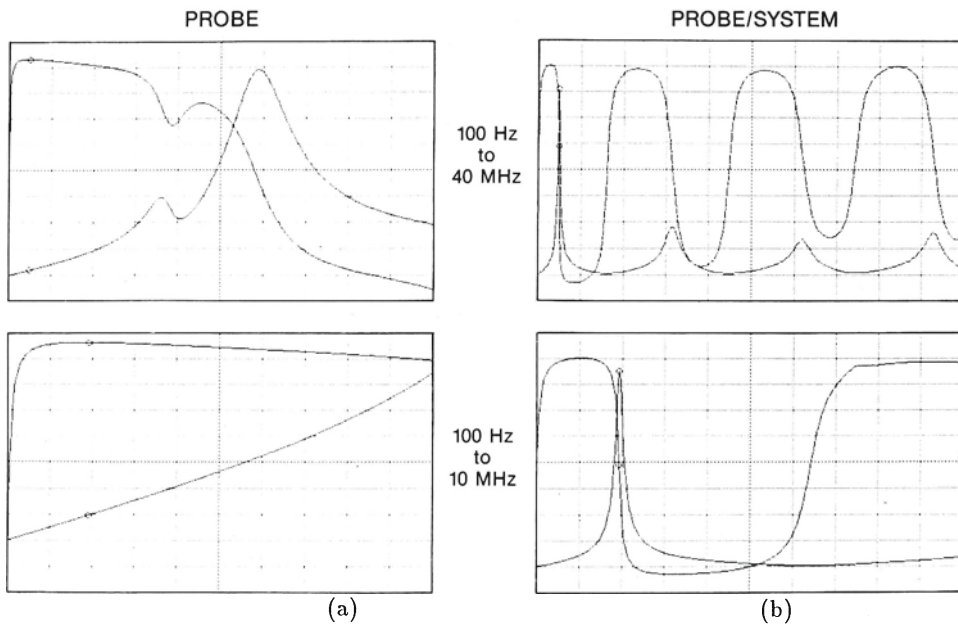


Figure 9. Frequency Response (a)probe (b)probe/system

graphs at the top in the figure show frequency response curves from 100 Hz to 40 MHz using an HP impedance analyzer. The bottom graphs are magnifications to show the response between 100 Hz and 10 MHz. The upper curves are the phase differences and the lower curves are the impedance magnitudes. To the left are the responses of the probe connected directly to the system and the resonance peak occurs at about 23 MHz. To the right are the responses when the probe is attached to a long cable and the resonance peak has dropped to 2 MHz which is right at the system operating frequency. No matter how good a probe is, the probe/system combination for this situation is very sensitive to noise.

In order to determine what the operating points should or should not be for the different probe designs, the added inductance and capacitance of the probe/system connection were measured. With these values added to the measured probe values, the probe/system resonance frequencies were then calculated and plotted, as shown in Figure 10. The proper operating frequency for each probe/system combination can then be selected. In general, the operating frequency should be on a gentle slope of the low frequency side of the resonance frequency peak. In particular, it is clear that probe design C should not be operated at 2 MHz for this particular probe/system combination.

Effects of varying probe diameter and velocity

Assuming that a good probe has been selected and the operating frequency is correct, there are still other parameters in the probe/system combination that affect detection sensitivity. Bolthole probes are adjusted to fit snugly in bolt holes to minimize liftoff effects by inserting a resilient shim into a cut in the probe plastic body and the question is how critical the fit is. An experiment was performed to determine what the probe diameter should be for optimum (meaning maximum signal to noise ratios) results when imaging a nominal 1/4" bolt hole with probe diameters from 246 mils to 262 mils. The probe diameter was carefully adjusted and measured with a micrometer before use and the system imaging conditions (gain and angle settings) were identical for each set of data. It is apparent from Figure 11a that

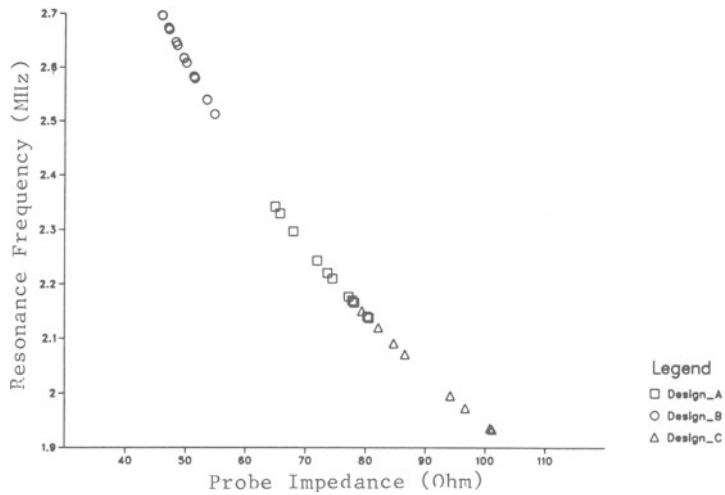
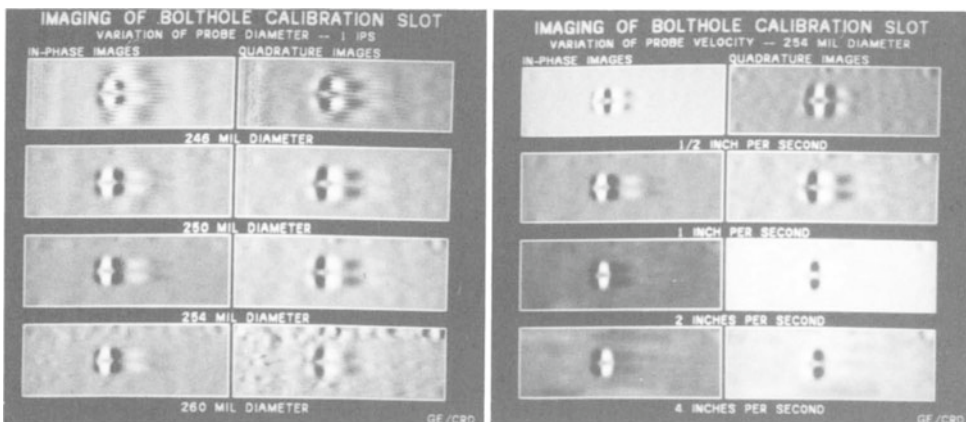


Figure 10. Probe/system resonance frequencies

there is an optimum diameter. A small diameter introduces noise in the image, most likely from excess vibration. With increasing diameter the noise is reduced and appears to be at a minimum at a diameter of 254 mils. As the diameter increases noise is again introduced, probably due to binding from the too tight fit of the probe in the bolt hole.

An experiment was also performed to determine what effect increasing the probe rotational velocity has on image data. Figure 11b shows images that were created at speeds of 1/2 ips (inches per second), 1 ips, 2 ips, and 4 ips using a near optimum probe diameter of 254 mils. Though the effect of a 5 Hz high pass filter is apparent in the images, the noise does not appear to increase drastically with increasing probe velocity for this diameter.



(a)

(b)

Figure 11. Variation of (a)probe diameter (b)probe velocity

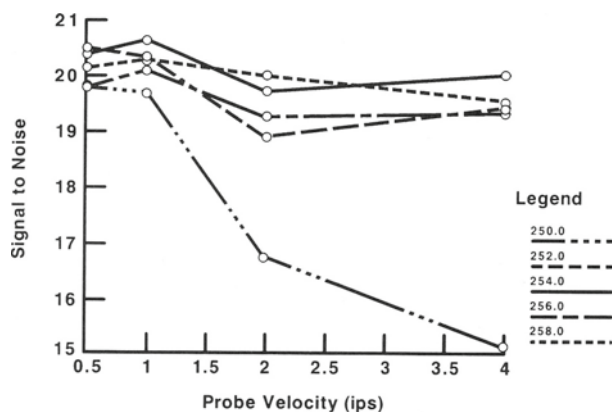


Figure 12. S/N ratios for different probe diameters and velocities

Signal to noise (S/N) calculations were performed on all images as a ratio between the peak-to-peak signal amplitude and the standard deviation of the image background. Figure 12 shows parametric curves of S/N of the magnitude data versus the probe diameter. It shows that a small diameter probe performs poorly with increasing speed but that the performances of larger diameter probes do not degrade drastically with increasing speed. According to the curves, 254 mils is the optimum probe diameter.

SUMMARY AND CONCLUSIONS

This paper has suggested new ways to analyze and improve the performance of eddy current inspections. In particular, a simple way of measuring the electric parameters of probes to evaluate their quality has been described. The results demonstrate that probe designs can be analysed to enable selection of probes with superior characteristics and to sort probes. Analysis of probe performance in an eddy current system and a method for selecting proper operating frequency also have been derived. Furthermore, the image footprint allows us to quantify what the actual active area of the probe is — information that has not been conveniently available before. This offers the ability to design probes and quantitatively evaluate the design. Finally, images were used effectively for system optimization experiments.

REFERENCES

1. K.H. Hedengren, R.O. McCary, and J.D. Young, "Use of Imaging Techniques for Eddy Current NDE", in *Review of Progress in Quantitative Nondestructive Evaluation*, edited by D.O. Thompson and D.E. Chimenti (Plenum Publishing Corporation, New York, 1988), Vol. 7A, pp. 357-365
2. R.E. Joynton, R.O. McCary, D.W. Oliver, K.H. Silverstein-Hedengren, and L.L. Thumhart "Eddy Current Imaging of Surface Breaking Structures," *IEEE Trans. on Magnetics*, Vol Mag-22, No. 5, Sept 1986